A study on point cloud interpretation of fracture intensity and its spatial variability

Yong-Zhi Huang
Department of Civil Engineering, National Taiwan University, Taipei, Taiwan

Tai-Tien Wang
Department of Civil Engineering, National Taiwan University, Taipei, Taiwan

Fu-Shu Jeng
Department of Civil Engineering, National Taiwan University, Taipei, Taiwan

ABSTRACT: In geological surveys with a rock engineering focus, the investigation and description of discontinuities is an important but time-consuming and labor-intensive step. With advances in surveying and mapping technology, digital surface models (DSM) and their corresponding point clouds can reproduce the geometric properties of outcrops, and provide a useful intermediary for rock fracture investigations. Here we develop and apply a method for fracture mapping that employs a discontinuity set extractor (DSE) program to capture fracture planes from point clouds and a spherical scan approach to determine fracture intensity in a direction-dependent fashion. The proposed approach is applied to obtain the fracture intensity of six outcrops, and the spatial variation of fracture intensity and corresponding influencing factors are investigated accordingly. The fracture intensity has both heterogeneous and directional-dependent characteristics. Their variations are affected by lithology and folds.

Keywords: Fracture intensity, Spatial variability, Advance surveying and mapping, Point cloud interpretation.

1 INTRODUCTION

Modern remote and sensing technologies, such as close-range photogrammetry and laser scanning, have advanced rapidly. A high-precision 3D outcrop point cloud model can be obtained by a terrain laser scanner, or be converted from the digital surface model (DSM) that can be generated using multipole photos taken from different angles. The DSM building process and corresponding point cloud model generation are now highly automated, leading these kinds of technologies are popularly carried out to help the engineering geology investigation (e.g. Xu et al. 2020 and Cirillo et al. 2022). To make good use of a point cloud model for rock outcrops, this study develops an approach for capturing geometric data of discontinuities based on the discontinuity set extractor (DSE) program (Riquelme et al. 2014). The fracture intensities of six outcrops in various rock types are then investigated, and their affecting factor are accordingly discussed hereafter.

2 3D OUTCROP POINT CLOUD MODELS

The DJI phantom 4 RTK is used to capture multiple photos for DSM generation. To enhance the accuracy of DSM, a distance of 10–20 m between the drone and the outcrop is maintained during the image capturing. Table 1 lists the information of produced DSMs, involving one metasandstone outcrop in Provincial highway No. 2, Taiwan, two outcrops of argillite interbedded with thin metasandstone layer in No. 7 highway and three highly metamorphic outcrops composed of metasandstone and slate in No. 20 highway. Figure 1 shows the corresponding point cloud models. The density of point ranges from 250–12690 pts/m^2.

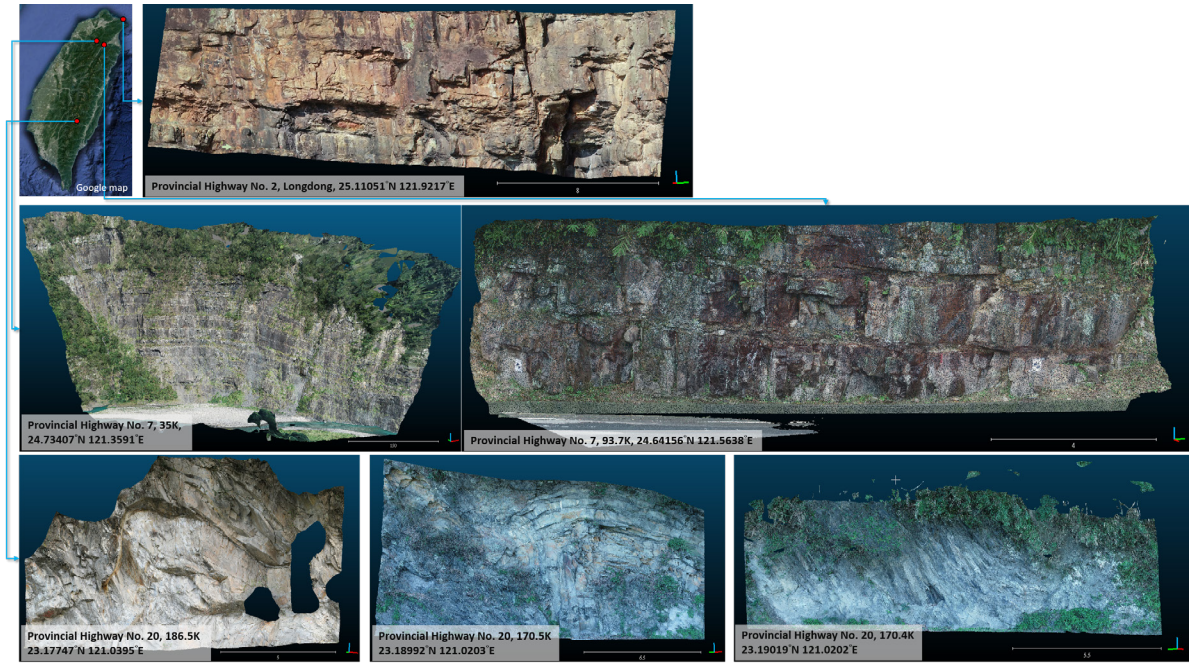

Figure 1. Location of six outcrops and point cloud model.

Table 1. Profiles of outcrop point cloud models.

Sites		25.11051°N 121.9217°E	24.73407°N 121.3591°E	24.64156°N 121.5638°E
Number of points	[pts]	2,987,109	1,857,036	489,216
Surface area	[m2]	235.4	7434	65
Density of points	[pts/m2]	12690	250	7526
Aspect/Dip	[°]	163/83	115/69	204/87
Sampling spacing	[m]	0.5	2.5	0.5
Sampling radius	[m]	0.5	2.5	0.5
Sampling number	[-]	744	925	183

Sites		23.17747°N 121.0395°E	23.18992°N 121.0203°E	23.19019°N 121.0202°E
Number of points	[pts]	900,862	804,746	346,837
Surface area	[m2]	122.7	110.2	46.5
Density of points	[pts/m2]	7342	7303	7459
Aspect/Dip	[°]	018/84	058/85	222/85
Sampling spacing	[m]	0.5	0.5	0.5
Sampling radius	[m]	0.5	0.5	0.5
Sampling number	[-]	315	360	143

3 INTERPRETATION OF FRACTURE INTENSITY

Figure 2 shows the proposed approach to obtain the fracture intensity P_{10} from outcrop point cloud model. First, points in specific locations are sampled to facilitate calculation time for P_{10} determination. Second, scanlines in various directions are generated with angle intervals of 10°. Third, the DSE code is implemented to extract the discontinuity information, and last, the P_{10} values corresponding to each scanline in each sampled point group are determined accordingly for subsequent discussion. Important procedures are introduced in the following.

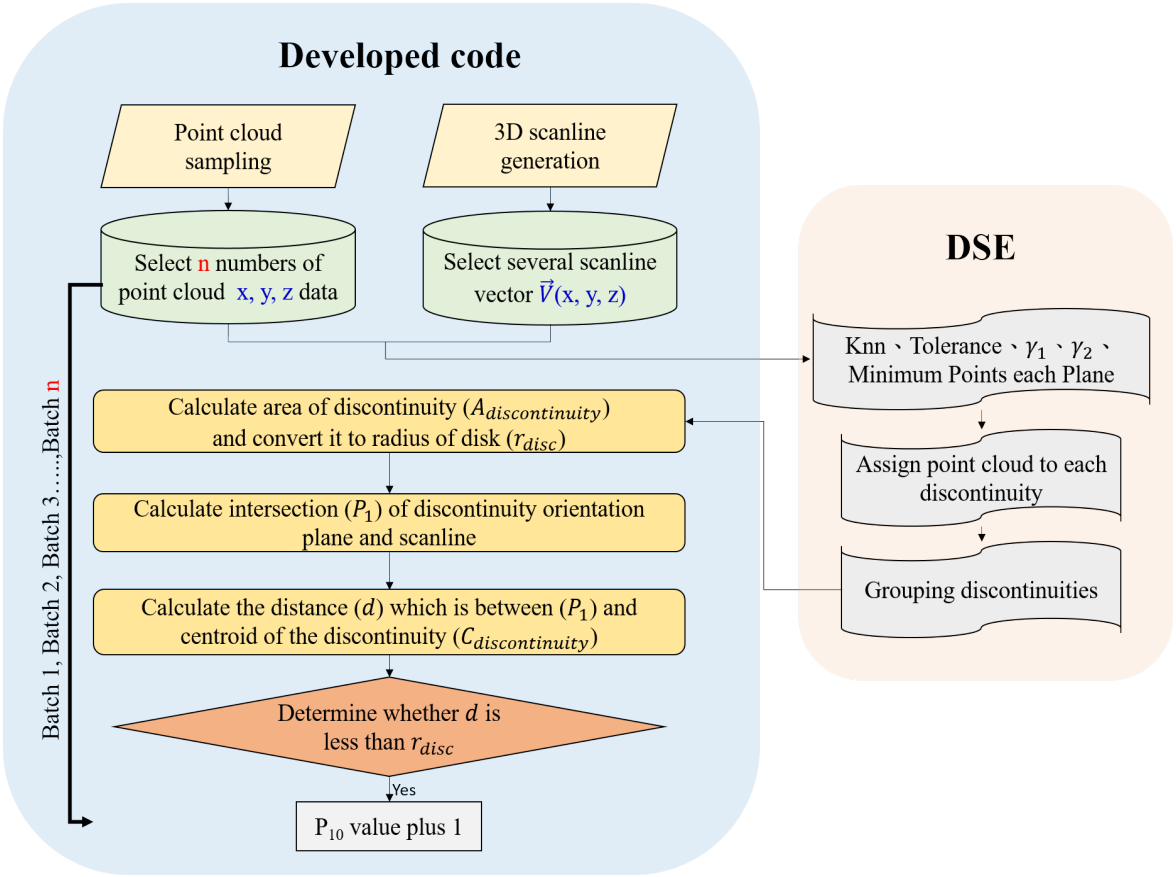

Figure 2. Process of P_{10} value calculation.

3.1 Fracture intensity P_{10} calculation

The defintion of P_{10} suggested by Mauldon et al. (2000), i.e., the number of fracture intersecting the scanline with unit length (with unit of L^{-1}), is referred to calculate the fracture intensity. Figure 3 shows the process of P_{10} calculation, visualized by the PyVista platform. First, all discontinuities are extracted by DSE, and converted into 3D discs with equal surface area (Figure 3(b)). Second, find point (P_1) which is the intersection between the discontinuity orientation plane and scanline (Figure 3 (c)). Third, compare the distance between point (P_1) to centroid of discontinuity ($C_{discontinuity}$) and radius of 3D disc (R_{disc}); if the former is less than latter then the P_{10} value will be recorded (Figure 3 (d)).

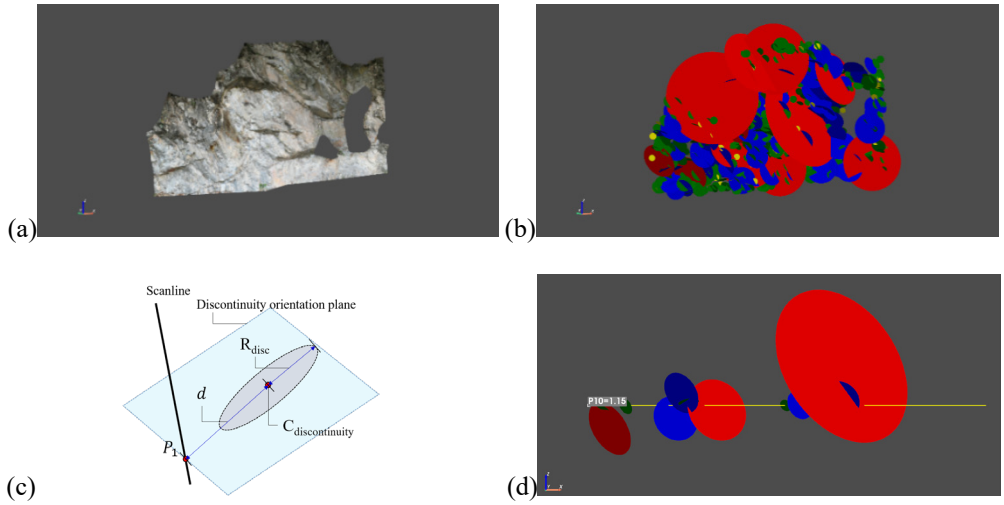

Figure 3. Scheme of P_{10} calculation. (a) Origin outcrop point cloud, (b) discontinuity converted to 3D disc, (c) geometry of 3D disc and scanline, (d) P_{10} results.

3.2 Point cloud sampling

The point cloud models of an outcrop typically consist of a huge number of x,y,z points. It is time consuming to interpret captured discontinuities for whole model calculation. Points in specific locations are sampled to ease such calculations (Figure 4). In this study, spheres of 1 m diameter with interval of 0.5 m are used for point cloud sampling. Notably, such sampling radius and interval are outcrop dependent.

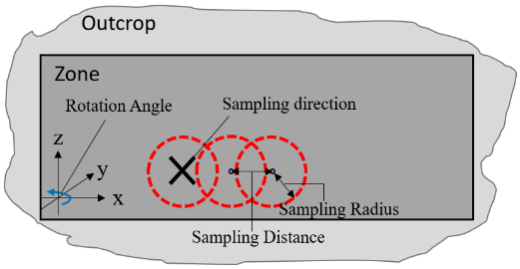

Figure 4. Point cloud sampling.

3.3 3D scanline generation

The direction of scanlines is described by two angles. The θ measures the zenith angle from the z-axis to y-axis on y-z plane (Figure 5(a)). Another θ_r measured the azimuth angle from the x-axis counter-clock wise in y-z plane (Figure 5(b-c)). For each P_{10} evaluation position, there are 307 scanlines since both the θ and θ_r have 10 degrees' intervals (Figure 5(d)).

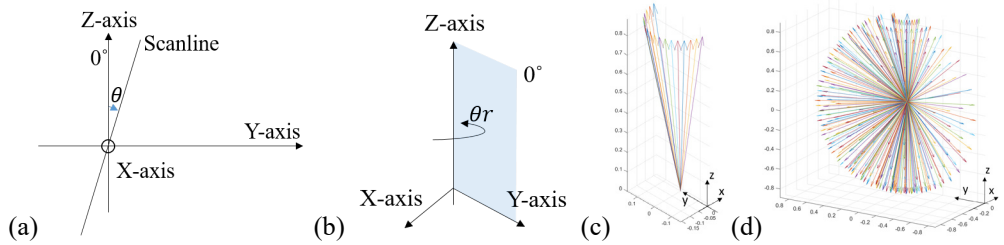

Figure 5. Definition of 3D scanline.

3.4 Fracture intensity P_{10} visualization

In addition to illustrate P_{10} along various directions of scanlines, the P_{10}s determined from the point cloud model are visualized on the original DSM. The P_{10} values are assigned to the center of the sampled sphere, and the inverse distance weighting (IDW) method is used to estimate P_{10} between sampling points, and some locations where point cloud is too sparely to determine P_{10}.

4 RESULTS

4.1 Fracture intensity P_{10} and variation

Taking the outcrop of Sta. 185.6 K, No. 20 highway as an example, Figure 6 shows the variation of P_{10} under various θ_r and θ. Each subfigure represents a scanline with specific combination of θ_r and θ, and $P_{10,\text{ all samples}}$ is the P_{10} summation of all samples, that means the results aren't affected by the number of samples and sample location, but effected by the scanline direction which are applied to the whole point cloud model through all samples. P_{10} values are higher when θ_r is 40°-60° and θ is 120°-140° (Figure 6), which are the appropriate directions for fracture intensity investigation.

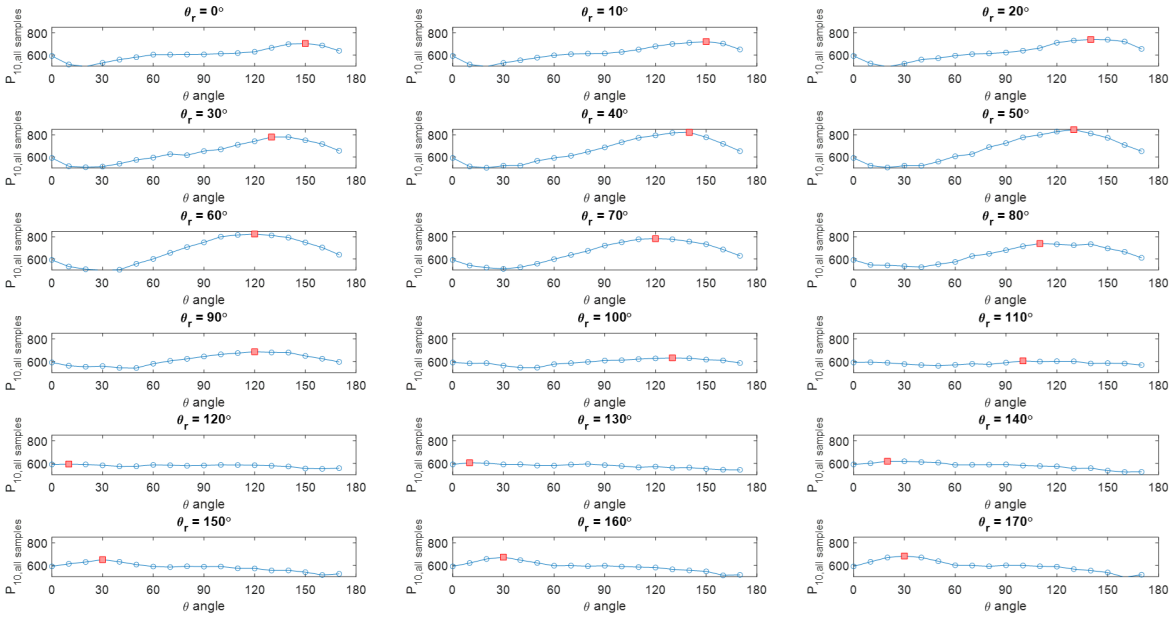

Figure 6. Sum of all samples P_{10} values with single scanline (Provincial Highway No. 20, 186.5K case).

4.2 Fracture intensity P_{10} spatial variation

After applying the P_{10} visualization method (section3.4), the $P_{10,\text{ all scanline}}$ graph is shown in Figure 7 and Figure 8. The $P_{10,\text{ all scanline}}$ is the sum of all scanline results for each sample, i.e., this value has no influence of directionality, but only depends on the location of the sample. In Figure 7 there is higher $P_{10,\text{ all scanline}}$ on the fold axis plane, and lower in both limbs. In Figure 8 the higher $P_{10,\text{ all scanline}}$ appears in the vicinity of the bedding plane and thinner layer.

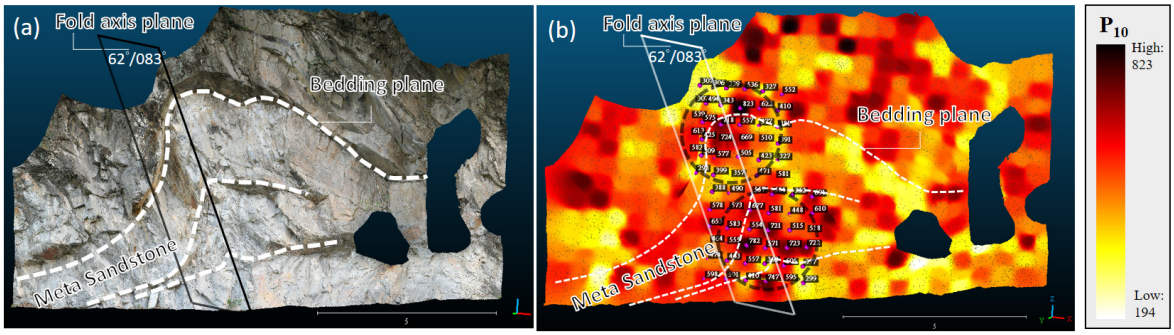

Figure 7. Provincial Highway No. 20, 186.5K case (a) Original point cloud (b) $P_{10,\text{ all scanline}}$ point cloud.

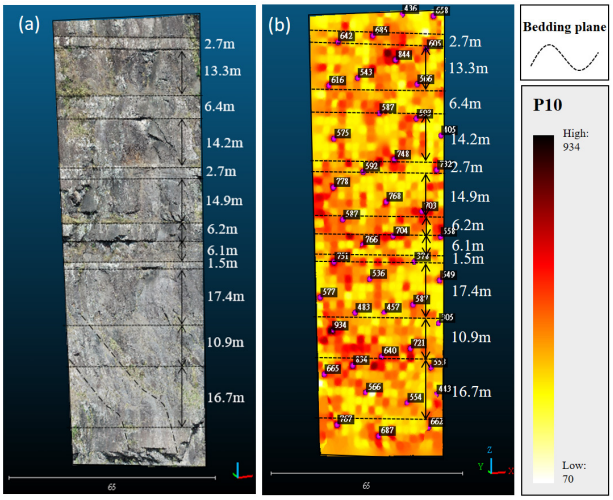

Figure 8. Provincial Highway No. 7, 35K case (a) Original point cloud (b) $P_{10,\text{ all scanline}}$ point cloud.

5 CONCLUSION

This study proposes a new approach to measuring fracture intensity from the outcrop point cloud model. The P_{10} value of a specific location and along various directions can be determined accordingly. Investigation results from six outcrops in various rock types with different geological structures indicate that P_{10} have strong spatial variability; both sampling position of point cloud and scanline direction significantly influence the determined magnitudes. For a specific site with a fold, P_{10} is higher near the fold axis plane, and lower in its both limbs. P_{10} is higher in the vicinity of bedding planes and thinner layer in the studied argillite/metasandstone interbedded formation.

REFERENCES

Cirillo, D., Cerritelli, F., Agostini, S., Bello, S., Lavecchia, G. & Brozzetti, F. 2022. Integrating Post-Processing Kinematic (PPK)–Structure-from-Motion (SfM) with Unmanned Aerial Vehicle (UAV) Photogrammetry and Digital Field Mapping for Structural Geological Analysis. *ISPRS International Journal of Geo-Information*, 11 (8), 437.

Mauldon, M. & Dershowitz, W. 2000. A Multi-Dimensional System of Fracture Abundance Measures. *Geological Society of America Annual Meeting.*

Riquelme, A. J., Abellán, A., Tomás, R., & Jaboyedoff, M. 2014. A new approach for semi-automatic rock mass joints recognition from 3D point clouds. *Computers & Geosciences*, 68, pp. 38-52.

Xu, W., Zhang, Y., Li, X., Wang, X., Ma, F., Zhao, J., & Zhang, Y. 2020. Extraction and statistics of discontinuity orientation and trace length from typical fractured rock mass: A case study of the Xinchang underground research laboratory site, China. *Engineering Geology*, 269 (105553)